PAPER • OPEN ACCESS

β-decay properties in the Cs decay chain

To cite this article: G. Benzoni *et al* 2018 *J. Phys.: Conf. Ser.* **966** 012024

View the article online for updates and enhancements.

IOP ebooks™

Bringing you innovative digital publishing with leading voices to create your essential collection of books in STEM research.

Start exploring the collection - download the first chapter of every title for free.

β-decay properties in the Cs decay chain

G. Benzoni

Istituto Nazionale di Fisica Nucleare, Sezione di Milano, I-20133 Milano, Italy

E-mail: giovanna.benzoni@mi.infn.it

R. Lică

ISOLDE-EP, CERN, CH-1211 Geneva 23, Switzerland
"Horia Hulubei" National Institute of Physics and Nuclear Engineering, RO-077125
Bucharest, Romania

M.J.G. Borge

ISOLDE-EP, CERN, CH-1211 Geneva 23, Switzerland
Instituto de Estructura de la Materia, CSIC, E-28006 Madrid, Spain

L.M. Fraile

Grupo de Física Nuclear, Facultad de CC. Físicas, Universidad Complutense, CEI Moncloa,
28040 Madrid, Spain

for the IDS collaboration.

Abstract.
    The study of the decay of neutron-rich Cs isotopes has two main objectives: on one side β decay is a perfect tool to access the low-spin structures in the daughter Ba nuclei, where the evolution of octupole deformed shapes can be followed, while, on the other hand, the study of the gross properties of these decays, in terms of decay rates and branching to delayed-neutron emission, are fundamental inputs for the modelling of the r-process in the Rare-Earth Elements peak. Results obtained at CERN-ISOLDE are discussed within this framework and compared to existing data and predictions from state-of-the-art nuclear models.

1. Introduction
Barium isotopes ($Z = 56$) are located in a region of the Segrè chart characterized by a variety of shape-related phenomena, including shape coexistence and possible static octupole deformation. High order deformations can have a strong influence on γ-decay rates and on quasi-particle energies, which are, in turn, inputs for the various theoretical models developed to describe these nuclei [1, 2].

    The interest in this mass region is not only based on the occurrence of exotic shapes, but also on the fact that these nuclei contribute to the peak of Rare-Earth Elements (REE). The origin of this peak, characteristic of the r-process, is still under debate: it can originate either via the
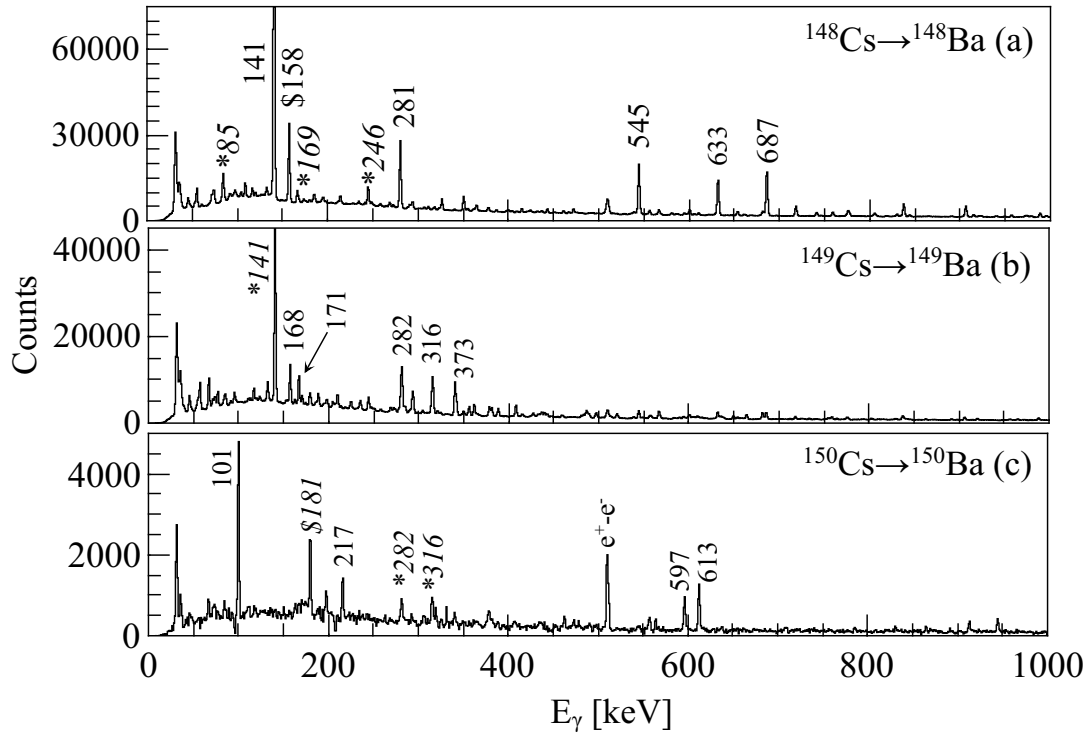
Figure 1. γ spectra following the ^{148}Cs$\rightarrow$^{148}Ba decay (top panel), following the decay ^{149}Cs$\rightarrow$^{149}Ba (central panel) and following the decay ^{150}Cs$\rightarrow$^{150}Ba (bottom panel). Transitions attributed to the main decay branches ($^{148-150}$Cs $\rightarrow$$^{148-150}$Ba) are indicated by their energies, while those corresponding to the βn branch by asterisks. The transition indicated by the dollar symbol belongs to the decay ^{149}Ba$\rightarrow$^{149}La. See text for more details.

r-process freeze-out stage when we have an equilibration of (n,γ) $\rightleftharpoons$ (γ,n) processes, or it can be fuelled by the fission of very heavy nuclei formed in merging stars [3, 4, 5].

In order to correctly model this process one has to provide a series of experimental quantities (fission, neutron capture, and β-decay rates), which are not easily accessible, given the very exotic nature of the parent nuclei.

2. Experimental details
In this work we study the β decays of $^{148-150}$Cs to $^{148-150}$Ba isotopes. The parent Cs isotopes have been produced at ISOLDE (CERN) [6, 7] by fission of a nano-structured UCx target induced by the 1.4-GeV proton beam delivered by the PS-Booster (PSB). The Cs atoms, thermally diffused out of the target matrix, were surface ionised and separated in the ISOLDE General Purpose Separator (GPS). The proton beam current ranged between $1.5 - 2\,\mu$A. Intensities of the exotic beams reaching the experimental setup were measured to be 5.5×10^2 ions/μC for mass A=148, 100 ions/μC for A=149 and 2 ions/μC for A=150 beam, taking into account a beamline transmission of $\sim$70%. The beam extraction was started 6 ms after the arrival of the proton pulse. Cs ions were implanted on an aluminised mylar tape at the center of the detection setup. The data acquisition recorded the arrival time of each proton pulse, using it as a reference for building decay curves. The tape was moved every 20-25 proton pulses (corresponding to a PSB super-cycle of $\sim$1 minute) in order to remove the unwanted daughter activity.

The experimental set-up consisted of the Isolde Decay Station (IDS), equipped with 3 fast-responding plastic scintillator detectors, to detect the β particles, 4 HPGe Clover detectors for the detection of γ rays following internal decay in the daughter nuclei, and 3 small-volume conic LaBr$_3$(Ce) detectors to perform lifetime measurements of specific nuclear states. The β detection array efficiency was 20% while the total HPGe efficiency, after add-back, amounted to 6% at 0.6 MeV. The digital processing of the energy signals yields resolutions at 1.3 MeV of the order of 2.3 keV for the HPGe detectors and 40 keV for the LaBr$_3$(Ce) ones. To increase the efficiency of the γ array no anti-Compton shield has been used, with HPGe crystals placed at few centimetres from the implantation point. The collected spectra show peaks due to partial depositions of energy by γ rays interacting via Compton or pair-production mechanisms.

Further details on the experimental set-up and analysis techniques can be found in Ref. [8, 9].

3. Results

Total γ spectra have been produced requiring a coincidence (ΔT) between the proton signal and the emission of a β particle, registered in the plastic scintillator. Different conditions, depending on the expected half-life, have been used for the three decays. In panel (a) of Fig. 1 we show the spectrum related to the decay ^{148}Cs→^{148}Ba, collected requiring ΔT<400 ms, in panel (b) the one corresponding to ^{149}Cs→^{149}Ba, collected in the same condition, and in panel (c) the one from the decay ^{150}Cs→^{150}Ba, collected in an interval ΔT<200 ms.

The main transitions attributed to each decay are indicated in the figure by their energy, while the ones marked by an asterisk, and whose energy is indicated in italics font, belong to the βn channel, which sizeably contributes to these decays, as it will be discussed later on. These transitions were used to extract the decay half-lives, which have been published in [8].

The extraction of the probability for emitting delayed neutrons (expressed in terms of P$_n$ values) is usually based on the ratio between the population of known states in the grand-daughter nuclei ^{A}Y and $^{A-1}$Y, taking into account the emission probability from the daughter, if known.

In the case of ^{148}Cs→^{148}Ba, being the βn successor (^{147}Ba) an even-odd nucleus its decay is characterised by a large fragmentation onto many final states. Three transitions are clearly seen in the spectrum at energies 85, 169 and 246 keV. The line at 158 keV belongs to the decay ^{148}La →^{148}Ce, coming as background from previous implantations, since the tape was moving every minute.

The ^{148}Cs neutron emission probability of P$_n$=38(4)% was determined from the ratio between the total number of ^{147}Ba and ^{148}Ba nuclei produced, estimated using the adopted values $I_{abs}(^{147}$La; 167.4 keV$) = 15.3(16)$% and $I_{abs}(^{147}$La; 196.1 keV$) = 6.7(7)$% [12].

In general, the decay from ^{149}Cs is fragmented onto many, closely lying, final states, and a strong contribution from delayed emission of neutrons is present. The βn branch seems to be mainly populating the 2^+ state in ^{148}Ba, even if a contribution from the $4^+ \rightarrow 2^+$ transition at 281 keV might be present. This second transition is hidden behind a γ transition at similar energy (282 keV) in the decay of ^{149}Ba.

The neutron emission probability, $P_n = 25(4)$% for ^{149}Cs, was extracted from the ratio of the total number of ^{148}Ba and ^{149}Ba nuclei using absolute γ-ray intensities in ^{149}Ba and βn daughters ^{148}La and ^{148}Ce. Literature values were used for I_γ (^{148}La; 415.8 keV$) = 3.6(1)$% [13] and I_γ (^{148}Ce; 158.5 keV$) = 56(1)$% [14].

In panel (c) two transitions can be identified as originating from the βn channel in the decay ^{150}Cs→^{150}Ba, at 282 and 326 keV. A third transition belongs to the successor's decay ^{149}Ba→^{149}La, indicated by the dollar symbol. In the case of the decay ^{150}Cs→^{150}Ba, the collected statistics is limited, and no previous experimental information on daughter decay are available. A ^{150}Cs neutron emission probability of P$_n$ <44(11)% was determined from the ratio between the total number of ^{149}Ba [8] and ^{150}Ba nuclei produced, estimated using the 316.6-
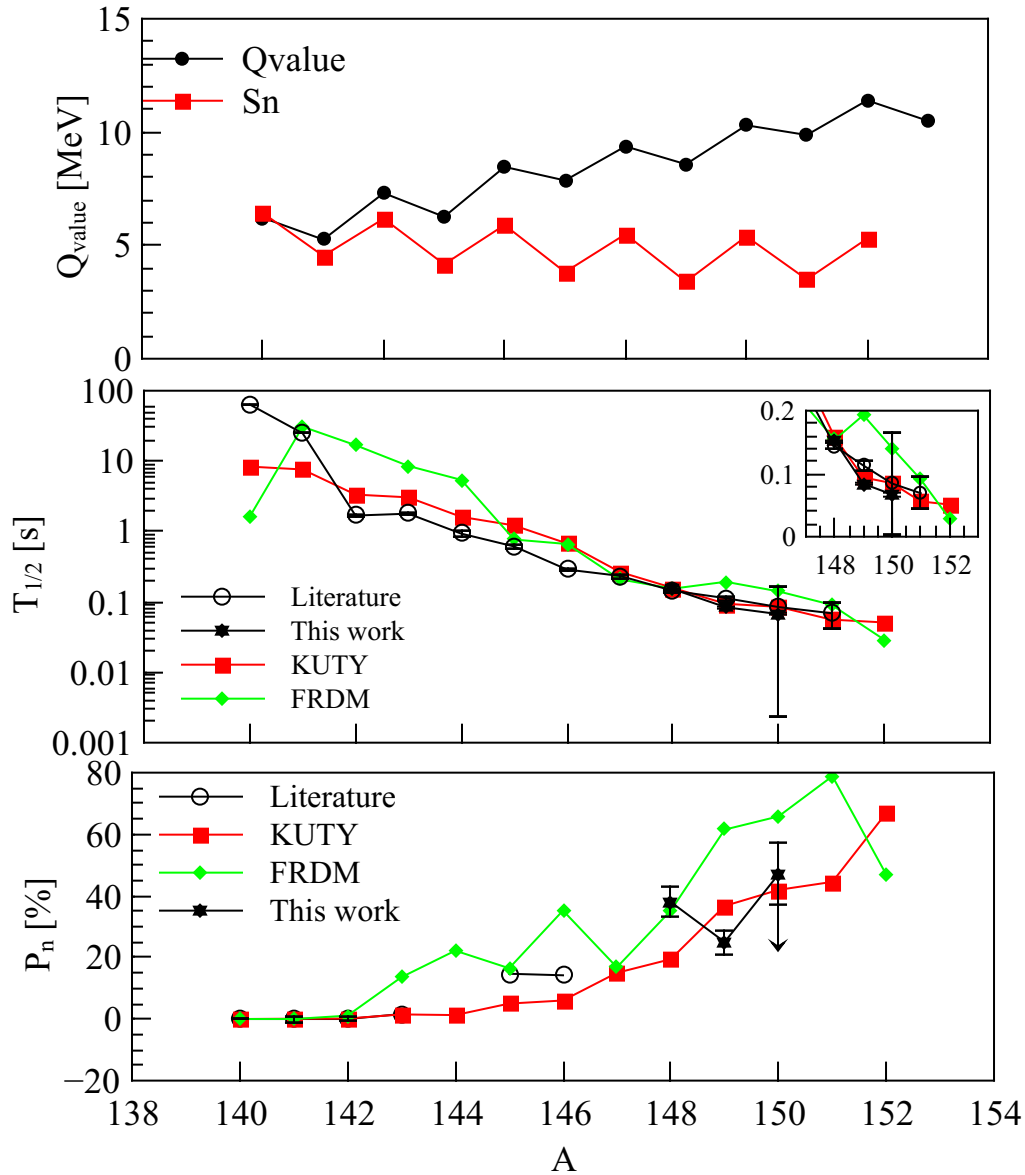
Figure 2. Top panel: Evolution of Q_β window (filled circles) and neutron separation energy (filled squares) as a function of mass in the Cs isotopic chain with A=140-152. The values are taken from the ENSDF database [10]. Central panel: Evolution of β-decay $T_{1/2}$: experimental values, shown by open circles, from masses A<144 are taken from the ENSDF database, while those for A≥144 from the recent compilation given in Ref. [11]. The experimental data obtained in this work are shown with filled stars. The data are compared with predictions obtained with KUTY (squares) and FRDM (diamonds) as described in the text. Bottom panel: evolution of P_n values (same symbols used in the middle panel).

and 101.1-keV transitions, respectively. For the transition at 101.1 keV a conversion coefficient of 1.86(3) [15] has been used, assuming a pure E2 character. We consider this as an upper limit, owing to the fact that we could not follow the decay to the grand-daughter.

4. Discussion

In this section we compare the extracted half-lives and P_n values with literature data and predictions coming from two of the most credited mass models available on the market.

The first is the finite-range droplet model (FRDM) which is based on quasi-particle random-phase approximation (QRPA). This model has been recently updated to include contributions also from first-forbidden transitions, in the framework of the statistical gross theory [16], which are expected to contribute $\approx 50\%$ of the total decay rate, with increased importance towards the most exotic species. The second model is based on the KUTY mass formula with the second generation of β-decay gross theory (GT2)[17]. Both models include the possibility of having deformed ground states, which are established to be present in this mass region [8, 9].

In the central panel of Fig. 2, we show the evolution of experimental and theoretical half-lives: The values extracted in this work, shown in the two panels with filled stars, are compared to experimental data (open circles) taken from literature: those referring to masses A<144 are taken from the ENSDF database [10], while for A$\geq$ 144 are from a recent measurement performed in Riken (J) during the EURICA campaign [11].

In the inset we expand the region where the two dataset can be compared: $T_{1/2}$ data extracted from our work are in general lower than the values extracted in Riken, even if they agree within the error bars. The large error bar for A=150 refers to the value reported in [11].

The data are compared with predictions obtained used the KUTY mass formula, shown in filled red squares and from the FRDM model in green diamonds.

Apart from the sudden jump seen for mass A=142, the $T_{1/2}$ data show a smooth decreasing trend, which is reproduced by both theories, with some slight deviations in the case of FRDM predictions.

At increasing mass we see, in the top panel of Fig. 2, that the Q_{value} window increases steeply, while the neutron separation energy, S_n, decreases smoothly. This opens the competition with the β-delayed neutron-emission channel, leading to the population of (A-1) species. The P_n values obtained in this work are again shown in filled stars, while the ones taken from literature with open circles. They are again compared with predictions from the previously described models.

We see that, up to ^{143}Cs $\rightarrow^{143}$Ba decay, the branching is negligible, while it becomes sizeable at mass around A=145. One should stress that experimental data points do not exist for all the decay chain. The comparison with theoretical predictions shows a better agreement with the description given by KUTY, while FRDM tends to overestimate the value by a large factor. The presence of strong non-axial deformations might affect the predictions for half-lives and P_n values.

[1] Butler P and Nazarewicz W 1996 *Rev. Mod. Phys.* **68** 349
[2] Robledo L M *et al.* 2010 *Phys. Rev. C* **81** 034315
[3] Mathews G J and Cowan J J 1990 *Nature* **345** 491
[4] R Surman J Engel J R B and Meyer B S 1997 *Phys. Rev. Lett.* **79** 1809
[5] M R Mumpower G C M and Surman R 2012 *Phys. Rev. C* **86** 035803
[6] Kugler E 2000 *Hyperfine Interactions* **129** 23
[7] Catherall J *et al.* 2017 *J. Phys. G: Nucl. Part. Phys.* **44** ..
[8] Lică R *et al.* 2017 *J. Phys. G: Nucl. Phys.* **44** 054002
[9] Lică R *et al.* submitted to *Phys. Rev. C*
[10] URL http://www.nndc.bnl.gov/ensdf/
[11] Wu J *et al.* 2017 *Phys. Rev. Lett.* **118** 072701
[12] Shmid M *et al.* 1981 *Proc.Int.Conf.Nuclei Far from Stability, Helsingor, Denmark* **2** 576
[13] Chung C *et al.* 1984 *Phys. Rev. C* **29** 592–602
[14] Gill R L *et al.* 1983 *Phys. Rev. C* **27** 1732–1744
[15] Kibédi T *et al.* 2008 *Nucl. Instr. and Meth. A* **589** 202–229
[16] Möller P, BPfeifer and Kratz K L 2003 *Phys. Rev.C* **67** 055802
[17] Koura H, Tachibana T, Uno M and Yamada M 2005 *Prog. Theor. Phys.* **113** 305